

Spectral bandwidth analysis of high sensitivity refractive index sensor based on multimode interference fiber device

Edwin G. P. Pachon^a, Marcos A. R. Franco^{b,c} and Cristiano M. B. Cordeiro^a

^aInstituto de Física "Gleb Wataghin" – IFGW, UNICAMP, Campinas, SP, Brazil

^bInstituto de Estudos Avançados – IEAv, São José dos Campos, SP, Brazil

^cInstituto Tecnológico de Aeronáutica – ITA, São José dos Campos, SP, Brazil

ABSTRACT

Fiber optic structures based on multimode interference were investigated to the refractive index (RI) sensing. The proposed device is a singlemode-multimode-singlemode (SMS) structure, where the multimode section is a coreless fiber (MMF). The numerical analyses were carried out by beam propagation and modal expansion methods. Ultra-high sensitivity was obtained: 827 nm/RIU over a RI range of 1.30–1.44 and a maximum sensitivity of 3500 nm/RIU for RI~1.43, considering $\Delta_{RI} = 0.01$. The dependence of spectral bandwidth was investigated taking into account the multimode fiber diameter and the coupling efficiency between modes at the input junction singlemode-multimode.

Keywords: Multimode interference, Refractive Index Sensor, Refractive Index Measurement, Fiber Optic Sensors

1. INTRODUCTION

Multimode interference (MMI) devices based on all-fiber have been used to build sensors for many physical parameters such as: temperature, pressure, strain, and refractive index [1]-[12]. Basically an all-fiber MMI device consists of a join of three optical segments: a step-index multimode fiber (MMF) spliced between two single-mode fibers (SMF), forming a SMS structure [1], [4], and [7]. The light coming from the input SMF excites several modes of the MMF section and, thus, causing interference among them along the fiber. The MMF length (L_{MMF}) is determined so that the interference pattern rebuilds the optical intensity and phase of the launch signal at start of the multimode region. The self-image occurs successive times along the MMF. If MMF section has these optimized lengths the self-image at output SMF provides a bandpass spectral peak. The lengths where the self-images occur depend on the: wavelength, MMF diameter, and the refractive index (RI) of the external medium at the MMF coreless region.

In this work, we present a SMS structure based on a pure silica coreless MMF section, with reduced diameter to improve the sensitivity of a refractometric sensor. The designs were numerically investigated by vectorial wide-angle beam propagation (BeamProp - Rsoft) and full vectorial modal expansion (FIMMPROP - Photon Design) softwares. Three SMS structures were considered allowing reaching an ultra-high sensitivity to RI variation. The influence of dimensional parameters of the MMF section over the RI sensor sensitivity and over the spectral transmission bandwidth is studied taking into account the number of excited modes at MMF and the coupling efficiency between the fundamental mode at the SMF and the modes at the MMF. In both input and output tips it was used a standard singlemode optical fiber (SMF-28) and between then a spliced coreless MMF section. Three MMF diameters were numerically considered: 125 μm , 78 μm , and 55 μm . The Figure 1(a) presents the typical geometric models of the SMS structures considering the three MMF diameters.

2. RESULTS

Figures 2(a)-(c) present the interferometric pattern in the xz plane for the SMS structure with MMF diameters (ϕ_{MMF}) of 55 μm , 78 μm , and 125 μm , respectively. For an external medium with refractive index $n_{liq}=1.0$ the length of first self-image is 11,373 μm , 22,801 μm , and 58,412 μm for ϕ_{MMF} of 55 μm , 78 μm , and 125 μm , respectively. The Figure 2(d) presents the normalized spectral transmission to the most sensible SMS structure, with $\phi_{MMF} = 55 \mu\text{m}$, as function of external RI. Figure 2(e) present the wavelength shifts at the maximal transmission peak as a function of the RI. The curve to $\phi_{MMF}=55 \mu\text{m}$ presents a better sensitivity with an average of 827 nm/RIU over a RI range of 1.30–1.44 [4]. To put this result in perspective we compare it with the result recently presented in [9], that uses a SMS structure with a tapered multimode section. The average sensitivity in our case is 1010 nm/RIU, two times higher than that obtained in [9] (~487 nm/RIU) to RI range of 1.33 to 1.44. A maximum sensitivity of 3500 nm/RIU is achieved for RI ~ 1.43, 80%

higher than that obtained in [9] (~1913 nm/RIU). The indexes in which the sensor exhibits maximum resolution are at indexes that are close to the index of the coreless MMF section.

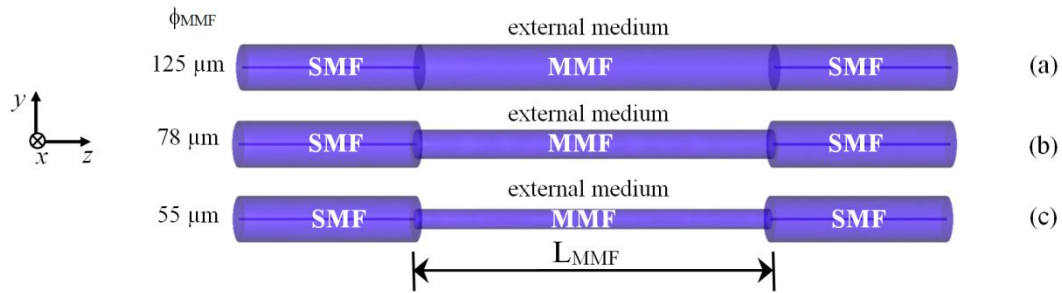


Figure 1. Multimode Interference SMS structure built with standard singlemode fiber (SMF28) and multimode coreless fiber (MMF). SMS structures with MMF diameters of 125 μm , 78 μm , and 55 μm .

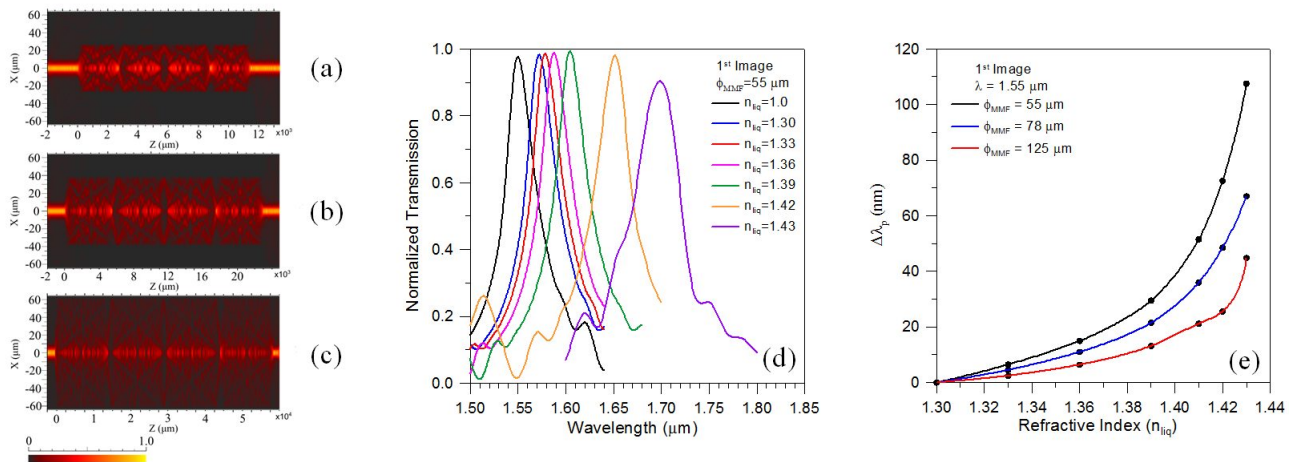


Figure 2. (a)-(c) Intensity distribution of optical power on the xz plane (transmission on z direction) at 1550 nm wavelength. (a) SMS structure with MMF diameter of 55 μm . (b) SMS structure with $\phi_{\text{MMF}} = 78 \mu\text{m}$. (c) SMS structure with $\phi_{\text{MMF}} = 125 \mu\text{m}$. (d) Spectral normalized transmission of SMS structure ($\phi_{\text{MMF}} = 55 \mu\text{m}$) to some different refractive indexes of the external medium. (e) Shifting of the maximum transmission wavelength peak (λ_p) as function of the RI change considering three diameters of MMF section.

The Figure 3(a) shows an example of modal coupling efficiency between the fundamental mode at SMF and the modes at MMF, as function of MMF diameter. The first six MMF radial modes are shown in Figure 3(b). The radial modes have higher coupling efficiency with SMF mode than the azimuthal modes, which has at least two orders of magnitude less efficiency. According to Figure 3(a), for $\phi_{\text{MMF}} = 55 \mu\text{m}$ the maximum coupling occurs to the second MMF mode - and the shape of the coupling efficiency curve is sharp involving just few modes. For ϕ_{MMF} equal to 78 μm or 125 μm , on the other hand, the coupling curve is smoother and involves more higher order modes.

The spectral transmission width increases as the core size of the MMF decreases or the external refractive index get closer to the fiber (silica) index - as some higher order modes are expected to be cutoff. The effect is more obvious for thinner fibers (55 μm) and higher refractive index ($n > 1.40$) external medium. Figure 4(b) show examples of spectral transmissions curves of SMS with $\phi_{\text{MMF}} = 55, 78$ and 125 μm , and $n_{\text{liq}} = 1.0$, where it is possible to observe the variation of bandwidth with the fiber diameter. The bandwidth also changes for different periodic self-images, reducing for high-order self-images (Figure 4(c)). A SMS device with high image resolution and good contrast is characterized by a narrow-peak (low bandwidth) and low ripple [13]. The bandwidth depends of the number of excited modes at MMF and the coupling efficiency curve between SMF-MMF modes (Figure 3(a)). If the coupling occurs just for few and lower order MMF modes, than the bandwidth is large. Otherwise, if many modes at MMF are excited the bandwidth becomes narrow.

Investigating the spectral transmission of SMS with $\phi_{\text{MMF}} = 125 \mu\text{m}$ and $n_{\text{liq}} = 1.0$, it was possible to observe the narrowing of the bandwidth when numerically more radial modes are considered at MMF. Assuming only three, five,

seven or ten radial modes, leads to decreasing values of FWHM to: 71, 27, 15, and 10 nm, respectively. To obtain the correct spectral transmission supported by the SMS it is necessary to use at least ten radial modes.

Despite the excellent sensitivity obtained to SMS with $\phi_{\text{MMF}} = 55 \mu\text{m}$, the FWHM is about 50 nm for the first self-image, and the resolution of a MMI sensor is inversely dependent of the transmission FWHM. Reducing the transmission bandwidth of the first self-image, allows to obtain more compact sensors with better resolution. To decrease the bandwidth is necessary to increase the coupling efficiency between modes at the junction SMF-MMF.

The Figure 5(a) presents the coupling efficiency of a SMS structure with $\phi_{\text{MMF}} = 55 \mu\text{m}$, in which the standard SMF was replaced for other single mode fibers with different numerical aperture (NA). Increasing the NA increases the acceptance angle and, in consequence, more higher modes are excited at the SMF-MMF interface. The Figure 5(b) shows the SMS spectral transmission considering four values of SMF numerical aperture: 0.1000, 0.1224, 0.1400, and 0.2400. The value NA=0.1224 corresponds to the standard SMF-28, used in all previous results in this work. The SMF with NA=0.2400 allows to obtain a FWHM of only 17.8 nm, a reduction of 64% in the FWHM.

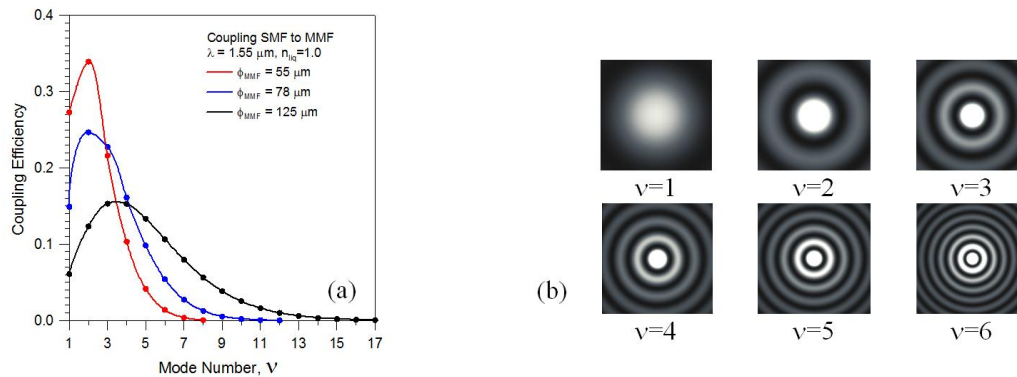


Figure 3. (a) Coupling efficiency between fundamental mode at singlemode fiber and fundamental and high order radial modes at multimode fiber. (b) Power distribution of the five first modes at MMF.

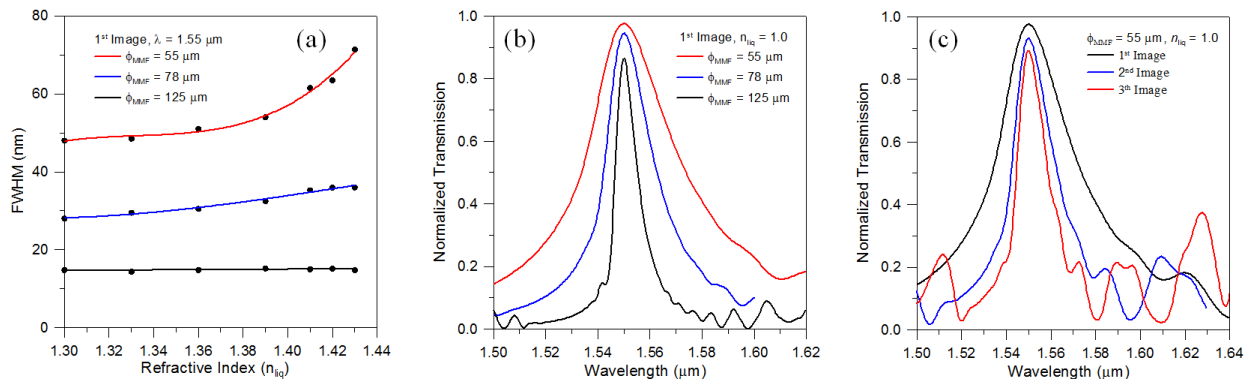


Figure 4. (a) Spectral transmission of the first image in SMSs structures with three different MMF diameters (55 μm , 78 μm , and 125 μm) considering $n_{\text{liq}} = 1.0$. (b) Full width half maximum (FWHM) of spectral transmission as function of the external medium refractive index. (c) Spectral transmission of the SMS with $\phi_{\text{MMF}} = 55 \mu\text{m}$ and $n_{\text{liq}}=1.0$, for the three first images formed at the MMF section.

3. CONCLUSION

This paper presents an interferometric device based on SMS structures and its application to RI sensing. The sensitivity was numerically evaluated to three diameters of MMF section, resulting in an ultra-high sensitivity for RI changes. The better result was obtained to $\phi_{\text{MMF}} = 55 \mu\text{m}$ allowing to reach an average sensitivity of $\sim 827 \text{ nm/RIU}$ over a RI range of 1.30–1.44 and a maximum sensitivity of $\sim 3500 \text{ nm/RIU}$ for RI ~ 1.43 , considering $\Delta_{\text{RI}} = 0.01$. To the best of our knowledge, this resolution is the highest reported to date for an all-fiber SMS based RI sensor.

The bandwidth of spectral transmission were investigated as function of RI change, MMF diameter, and number of MMF excited modes. It was observed a correspondence between the spectral bandwidth of SMS transmission and the maximum number of the MMF supported modes and also with the modal coupling efficiency at SMF-MMF interface. The analysis indicates that the adequate choice of MMF dimensions allows to improve the SMS resolution to obtain a narrow spectral transmission suitable for high resolution and high sensitivity sensor.

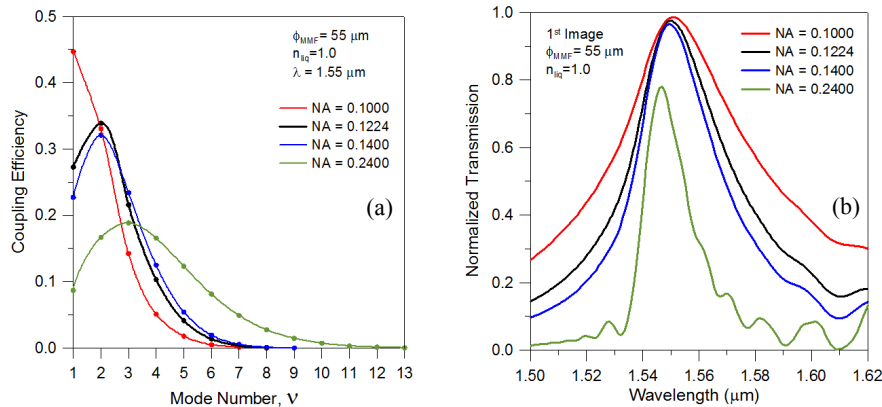


Figure 5. Spectral transmission of SMS structures with $\phi_{MMF} = 55 \mu\text{m}$, considering different number of excited MMF modes.

ACKNOWLEDGMENTS

This work was partially supported by project Pró-Defesa CAPES/Ministério da Defesa (ref. 23038.029912/2008-05), Finep (ref 0.1.06.1177.00, 0.1.05.0770.00, 1986/09, and 1894/10), CNPq and FAPESP by project INCT Fotonicom.

REFERENCES

- [1] Aguilar-Soto, J. G., Antonio-Lopez, J. E, Sanchez-Mondragon, J J, and May-Arrijoa, D. A., " Fiber Optic Temperature Sensor Based on Multimode Interference Effects," Proceedings of XVII Reunión Iberoamericana de Óptica & X Encuentro de Óptica, Láseres y Aplicaciones, Journal of Physics: Conference Series 274, pp. 1-4, (2011).
- [2] Linh Viet Nguyen, Dusun Hwang, Suhei Moon, Dae Seung Moon, and Youngjoo Chung, " High temperature fiber sensor with high sensitivity based on core diameter mismatch," Optics Express, vol. 16, No. 15, pp. 11369-11375, (2008).
- [3] Hatta, A.M., Rajan, G., Semenova, Y. and Farrell, G., " SMS fibre structure for temperature measurement using a simple intensity-based interrogation system," Electronics Lett., vol. 45, No. 21, (2009).
- [4] Silva, S., Pachon, E. G. P., Franco, M. A. R., Hayashi, J. G., Malcata, F. X., Frazão, O., Jorge P., Cordeiro, C. M. B., " Ultra-High Sensitivity-Temperature Fiber Sensor Based on Multimode Interference," Applied Optics (accepted to publication).
- [5] Wang, P., Brambilla, G., Ding M., Semenova, Y., Wu, Q., and Farrell, G. "Investigation of single-mode–multimode–single-mode and single-mode–tapered-multimode–single-mode fiber structures and their application for refractive index sensing," J. Opt. Soc. Am. B / Vol. 28, No. 5, pp. 1180-1186, (2011).
- [6] Wu, Q., Semenova, Y., Wang P., and Farrell G., "High sensitivity SMS fiber structure based refractometer – analysis and experiment," Optics Express, vol. 19, No. 9, pp. 7937-7944, (2011).
- [7] Jin, Y. X., Chan, C. C., Zhao, Y., Dong, X. Y., " Refractive index measurement by using multimode interference," Proceedings of 21st International Conference on Optical Fiber Sensors, Proc. of SPIE vol. 7753, 77535F, (2011).
- [8] Zhang, C., Li, E., Peng L.V., Wang, W., " A wavelength encoded optical fiber sensor based on multimode interference in a coreless silica fiber," Proceedings of International Conference on Optical Instruments and Technology: Advanced Sensor Technologies and Applications, Proc. SPIE SPIE Vol. 7157, 71570H, (2009).
- [9] Wang, P., Brambilla, G., Ding, M., Semenova, Y., Wu, Q., and Farrell, G., "High-sensitivity, evanescent field refractometric sensor based on a tapered, multimode fiber interference", Opt. Lett., 36, 2233–2235 (2011).
- [10] Mehta, A., Mohammed, W., and Johnson, E. G., "Multimode interference-based fiber-optic displacement sensor", IEEE Photon. Technol. Lett., 15, 1129–1131 (2003).
- [11] Hatta, A. M., Semenova, Y., Wu, Q., and Farrell, G., "Strain sensor based on a pair of single-mode-multimode-single-mode fiber structures in a ratiometric power measurement scheme", Appl. Opt., 49, 536–541 (2010).
- [12] Silva, S., Frazão, O., Viegas, J., Ferreira, L. A., Araújo, F. M., Malcata, F. X., and Santos, J. L., "Temperature and strain-independent curvature sensor based on a singlemode/multimode fiber optic structure", Meas. Sci. Technol., 22, 085201 (2011).
- [13] Soldano, L. B., Pennings, E. C. M., "Optical multi-mode interference devices based on self-imaging: principles and applications," J. Lightwave Technol., vol.13, No. 4, pp. 615-627, (1995).